Task-Based and Stable Tele-Nanomanipulation in a Nanoscale Virtual Environment

Sung-Gaun Kim, *Member, IEEE* and Metin Sitti, *Member, IEEE*

***Abstract*— In a haptic interface system with a nanoscale virtual environment (NVE) using an atomic force microscope (AFM), not only stability is important but also task-based performance (or fidelity) is crucial. In this paper, we introduce a nanoscale virtual coupling (NSVC) concept and explicitly derive the relationship between performance, stability and scaling factors of velocity (or position) and force. An available scaling factor region is represented based on Llewellyn's absolute stability criteria and the physical limitation of the haptic device. For the stable haptic interface, the sampled time passivity controller is implemented in the NVE. Experiments have been performed for tele-nanomanipulation tasks such as positioning, indenting and nanolithography with guaranteed stability in the NVE.**

***Index Terms*— Haptic interfaces, nanorobotics, teleoperation control, nanotechnology**

I. Introduction

Tele-nanomanipulation enables a human operator to interact with the nano world where she/he cannot physically exist. Manipulating a nanoscale object is a challenging task that is beyond the capabilities of human sensing and precision. Since surface forces and intermolecular forces dominate over gravitational and other more intuitive forces of the macro world at the nanoscale, a user is not familiar with these novel nanoforce effects [1].

In order to overcome this scaling barrier, human machine interfaces that consist of visual, tactile or force feedback at the macro world have been used with an Atomic Force Microscope (AFM) as a manipulator at the nanoscale [1], [2]. Force reflecting perception is important not only for enriching human operators to indirectly feel interaction between an AFM probe tip and samples at the nanoscale, but also for reliable telemanipulation of fragile, soft and complex nonoobjects such as biological samples or polymers. Hollis *et al*. [2] used a Scanning Tunneling Microscope (STM) as the nanomanipulator with a haptic device for teleoperated nanoscale topography feedback. Falvo *et al*. [3] and Guthold *et al*. [4] also used an AFM as the nanoManipulator with a haptic interface.

Due to lack of real-time visual feedback during AFM nanomanipulation, virtual reality with human machine interfaces for tele-nanomanipulation were developed by some researchers [3]-[7]. Vogl *et al*. [5], [6] and Li *et al*. [7] presented augmented reality to enrich human machine interface for manipulation of nanoscale objects with AFM. In addition, this nanoscale virtual environment (NVE) is beneficial for learning or performing nanoscale tasks such as nanofabrication [8] and cell manipulation [9]. Also, the NVE provides a useful tool for researchers in a variety of disciplines such as biology, chemistry and physics. Moreover, it may even be used for educational purposes. Hence, we focus on the interaction with the NVE using haptic device.

However, previous studies have not considered the stability and the task-based performance when operators have tasks using haptic interfaces in the NVE. Moreover, the selection of scaling factors was not explicitly discussed. Therefore, we investigate methods and control schemes for the task-based and stable tele- nanomanipulation in the NVE in this study.

In haptic interface systems stability is an important issue [10]-[14]. In the NVE simulation, instability can cause the operator to feel an undesirable force feedback (such as unnecessary oscillation of the haptic device) distorting the transparent interaction with the NVE. This instability can be dangerous if the haptic device is capable of instantaneous high force output. It is attributed to overlap of continuous time, discrete time, and sample time in haptic interface. Haptic rendering operates in discrete time from sampled position lag behind actual position in the NVE. For the stability in haptic interface, Colgate and Schenkel [10] introduced a virtual coupling concept using passivity theorem. Adams and Hannaford [11] also implemented the virtual coupling in order to guarantee haptic interface stability in their system. Ryu *et al*. [13] suggested a time domain passivity control in order to dissipate the excess energy generated by instability. This time domain passivity approach could be simply implemented without exact knowledge of the environment dynamics.

Compared to conventional haptic interfaces with a hard contact virtual environment, haptic exploration with the NVE, such as AFM with tapping (or intermittent contact) mode operation, nanofabrication and cell manipulation requires a very high level of performance (or fidelity). Cavusoglu *et al*. [14] proposed a new fidelity measure based on the sensitivity of transmitted impedance changes for soft environments. Colgate

Manuscript received November 2004.

Sung-Gaun Kim is with the Mechanical and Automotive Engineering Department, Kongju National University, 182 Shinkwan-dong, Kongju, 314-701, Korea (corresponding author to provide phone: +82-41-850-0611; e-mail: kimsg@kongju.ac.kr).

Metin Sitti is with the Mechanical Engineering Department and Robotics Institute, Carnegie Mellon University, PA 15213, USA (e-mail: sitti@cmu.edu).

and Brown [15] suggested a dynamic range of achievable impedance, namely *Z-width*, to measure the performance of force reflecting interfaces.

In this paper, we introduce the nanoscale virtual coupling (NSVC) concept to present the scaling effects between the macroscale and nanoscale worlds. The *Z-width* of NSVC based on hybrid matrix [11] is investigated to represent the performance of tele-nanomanipulation for a given task. Also, we explicitly derive the relationship between performance, stability, and impedance scaling factors. Available scaling factor region of NSVC is represented using Llewellyn's absolute stability criteria and the physical limitation of the haptic device. Based on the sampled time domain passivity control theory, the stable haptic interface is implemented in the NVE. An *Omega*® haptic device made by Force Dimension Inc. is used for verifying the stable control schemes in the developed NVE. Experiments with the haptic device have been performed for tele-nanomanipulation tasks such as indenting and nanolithography with guaranteed stability.

This paper is organized as follows; Section II describes the tele-nanomanipulation system overview. Section III proposes NSVC and the tele-nanomanipulation control law with guaranteed stability. In addition, the relationship between performance, stability and impedance scaling is discussed. The next section presents results of experiments to verify the proposed task-based and stable control scheme. Section V presents conclusions and future investigations.

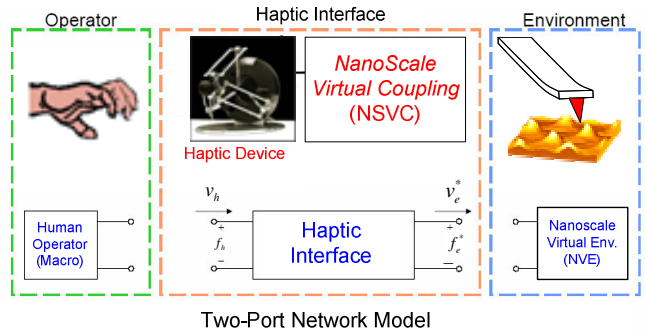

Fig. 1. Tele-nanomanipulation overall system as a two-port network model

II. System Overview

In this section, we present the overall tele-nanomanipulation system that is composed of human operator, haptic interface and NVE. Fig. 1 shows the three primary elements in a two-port network model of haptic simulation [11].

A. Operator

It is assumed that the human operator should be unable to destabilize the system by modulating limb impedance using muscular contraction or changes in musculoskeletal pose (geometry) [11]. In other words, we can assume the human operator to be passive at frequencies of interest. According to Hogan's experimental studies, he investigated that despite neural feedback within the arm and a high degree of adaptability in the neuromuscular system, the impedance exerted by a human is passive [20]. Thus, it is a reasonable assumption that we should consider the energetic interaction between the human arm and a mechanical device as passive.

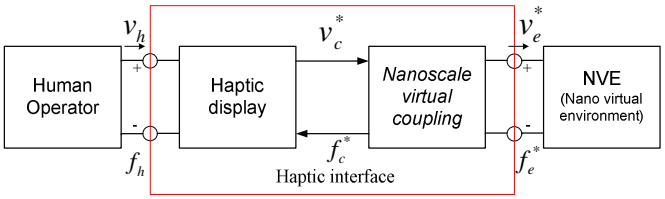

Fig. 2. Tele-nanomanipulation with haptic interface

B. Haptic Interface

The haptic interface part in Fig. 2 consists of the haptic display and NSVC. Fig. 3 shows that the *Omega*® haptic device (or display) is connected to the nanoscale contact surface of NVE through a NSVC with additional damper. In this figure, the v_c^* is an output of the haptic device and f_c^* is an input of haptic display. The parameters with '*' are in discrete form. Note that the NVE is the *impedance display* that the position (or velocity) is an input and force is an output. The *Omega*® haptic device based on parallel *delta robot* mechanism has 3 degrees of freedom (x, y, z position in Cartesian space). The workspace of the haptic device can completely hold an 88mm cube. The maximum continuous force in Cartesian space depends on the direction of exerted force and position in the workspace. The best case is around 20N and the worst case is around 8N. Since this haptic device has the ability to compensate for gravity for the human operator, it is suitable for force reflecting perception and interaction with NVE.

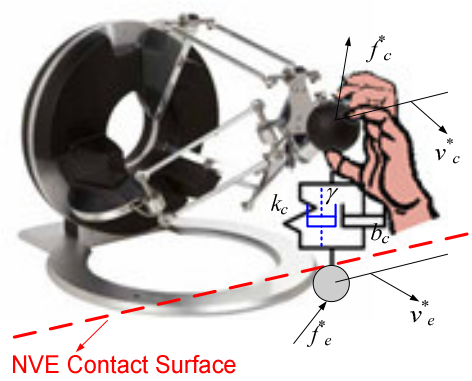

Fig. 3. Nano scale virtual coupling (NSVC) – spring and damper model

C. Nanoscale Virtual Environment

The NVE is developed for the interaction between AFM probe and nano surface shown in Fig. 4. The AFM tip is described as a sphere and a nano sample surface is presented in the left part of Fig. 4. The cone on top of AFM tip sphere presents forces exerted on the tip. Also, the visualized cantilever that shows the deflections of the cantilever and the positions and forces of AFM tip were presented in Fig. 4.

A linear bending beam model has been used for the behavior

of the probe and a *spline* based model has been developed for the nano sample surface upon which a collision detection algorithm determines. A Maugis-Dugdale (MD) contact mechanics model and non-contact nanoforce (van der Waals forces and capillary forces) models [1], [5], [6] are combined to simulate the interaction between the AFM tip and sample (see Fig. 5).

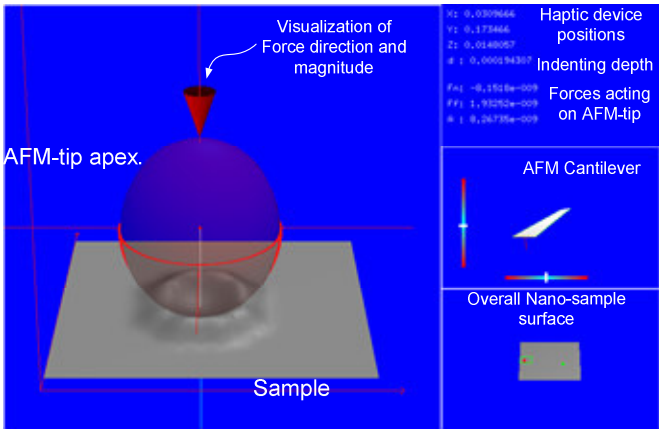

Fig. 4. Nanoscale virtual environment experiment for telemanipulation

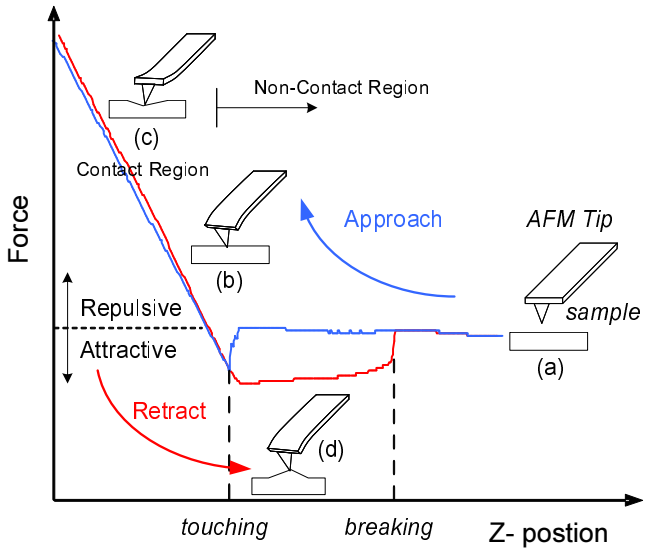

Fig. 5. Non-contact and contact MD force models in the NVE (See Fig. 6)

III. Tele-Nanomanipulation Control

A. Hybrid Matrix

Consider the tele-nanomanipulation control architecture as shown in Fig. 7. Here, the haptic interface can be modeled as a two-port network element. The operator and environment dynamics are modeled by Thevenin equivalents having impedances $Z_h(s)$ and $Z_e(z)$, and exogenous force inputs [16] f_h^a and f_e^a, respectively:

$$f_h = f_{h\_a} - Z_h(s)v_h$$
$$f_e^* = f_{e\_a}^* + Z_e(z)v_e^* \quad (1)$$

where v_h and v_e^* are the human and nanomanipulator velocities, respectively. f_h is the force applied by operator on the master, and f_e^* is the force applied by the virtual AFM tip in the NVE.

The *Omega*® haptic device dynamics are discretized using Tustin's method which preserves the passivity of impedance function [11],

$$Z_d(z) = (ms+b)\Big|_{s\to\frac{2}{T}\left(\frac{z-1}{z+1}\right)} \quad (2)$$

It is assumed that any aliasing effects are negligible. Also the sampler can be approximated as a static gain of $1/T$.

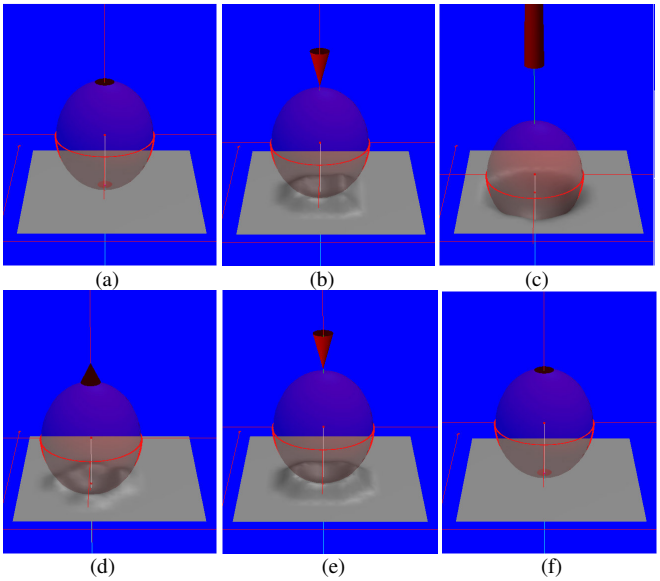

Fig. 6. Nanoforce visualization during AFM tip approach / retraction (see Fig. 5)

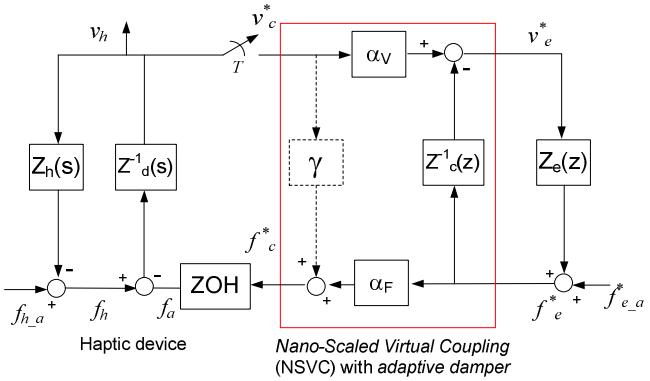

Fig. 7. The tele-nanomanipulation control architecture

The discrete hybrid matrix of the haptic display can be expressed as

$$\begin{bmatrix} f_h \\ -v_c^* \end{bmatrix} = \begin{bmatrix} Z_d(z) & ZOH(z) \\ -1 & 0 \end{bmatrix} \begin{bmatrix} v_h \\ f_c^* \end{bmatrix} \quad (3)$$

where zero-order hold function can be expressed as

$$ZOH(z) = \frac{1}{2}\frac{(z+1)}{z}$$

In the proposed tele-nanomanipulation control architecture, forces and velocity (or position) signals being communicated between the haptic device and the NVE are as follows:

$$v_e^* = \alpha_v v_c^* - \frac{1}{Z_c(Z)} f_e^*$$

$$f_c^* = \begin{cases} \alpha_F f_e^* \\ \alpha_F f_e^* + \gamma v_c^* \end{cases} \quad \text{if adaptive damper is active.} \tag{4}$$

where α_v and α_F are the velocity and force scaling factor, respectively. Z_c and γ are the virtual coupling impedance and the additional adaptive damper for the stability, respectively. Discretization of virtual coupling impedance can be derived using a first difference approximation,

$$Z_c(z) = \left(b_c + \frac{k_c}{s} \right)\Bigg|_{s \to \left(\frac{z-1}{Tz}\right)} \tag{5}$$

Therefore, the hybrid mapping of the NSVC network (if adaptive damper is active) is

$$\begin{bmatrix} f_c^* \\ -v_e^* \end{bmatrix} = \begin{bmatrix} \gamma & \alpha_F \\ -\alpha_v & \frac{1}{Z_c(z)} \end{bmatrix} \begin{bmatrix} v_c^* \\ f_e^* \end{bmatrix} \tag{6}$$

Finally, we can derive the hybrid mapping for the haptic interface that is the cascade connection of the impedance display with the NSVC network,

$$\begin{bmatrix} f_h \\ -v_e^* \end{bmatrix} = \begin{bmatrix} Z_d(z) + \gamma \cdot ZOH(z) & \alpha_F \cdot ZOH(z) \\ -\alpha_v & \frac{1}{Z_c(z)} \end{bmatrix} \begin{bmatrix} v_h \\ f_e^* \end{bmatrix} \tag{7}$$

B. Performance (Transparency or Fidelity)

The term 'transparency' or 'fidelity' is defined to describe the similarities in terms of "*feeling*" between performing a task with the teleoperator and performing the same task manually or directly without the teleoperator. The performance of a haptic interface can be described in terms of transparency in which velocities and forces are passed between the human operator and the NVE. One form of transparency measure is proposed by Colgate and Brown [15] as the notion of impedance range. This is delimited by frequency dependent minimum and maximum impedance bounds which the haptic interface can stably render to the human operator. Therefore, performance of the haptic interface can be expressed in terms of lower and upper bounds on the impedance perceived (or transmitted) by the human operator, Z_t .

By terminating the NVE port in Fig. 7, $f_e^* = Z_e(z) v_e^*$, the environment impedance(Z_e) transmitted through haptic interface(Z_t) can be derived as

$$Z_t = (Z_d(z) + \gamma \cdot ZOH(z)) + \frac{\alpha_v \alpha_F \cdot Z_c(z) \cdot ZOH(z) Z_e}{Z_c(z) + Z_e} \tag{8}$$

The lower bound on *Z-width* [15] can be derived as (by letting $Z_e \to 0$, i.e. $f_e^* = 0$, short circuit)

$$Z_{t,\min} = Z_d(z) + \gamma \cdot ZOH(z) \tag{9}$$

The upper bound impedance is found by letting $Z_e \to \infty$ (i.e. $v_e^* = 0$, open circuit).

$$Z_{t,\max} = (Z_d(z) + \gamma \cdot ZOH(z)) + \alpha_v \alpha_F \cdot Z_c(z) \cdot ZOH(z) \tag{10}$$

Therefore, *Z-width* can be defined as

$$Z_{t,\max} = Z_{t,\min} + \alpha_v \alpha_F \cdot Z_c(z) \cdot ZOH(z) \tag{11}$$

The *Z-width* can be expressed in terms of *impedance scaling factor* ($\alpha_v \alpha_F$) and *virtual coupling impedance* ($Z_c(z)$). Hence, the nanoscale virtual coupling (NSVC) can be defined as,

$$NSVC = \alpha_v \alpha_F \cdot Z_c(z) \tag{12}$$

In order to improve performance with respect to human perceptual capability, it is reasonable to build a single programmable haptic interface which can exhibit a comparable broad dynamic range of impedance (*Z-width*). To maximize *Z-width*, we should maximize impedance scaling factor ($\alpha_v \alpha_F$) or virtual coupling impedance ($Z_c(z)$). In other words, for the best performance, high impedance scaling factor, virtual stiffness, and virtual damping should be as large as possible. If the haptic interface is absolutely stable [11], then *Z-width* means an upper and lower bounds on realizable impedance. In Section III.*D*, we will discuss how the impedance scaling factor affects *Z-width*.

C. Stability: Sampled Time Domain Passivity Approach

The stability of haptic interactions is crucial because unwanted oscillations are deteriorating the haptic sense and potentially unsafe for the human operator. In order to guarantee stable haptic interface, we use the sample time domain passivity approach [13].

If the energy of the system increases with time when perturbed from equilibrium, the system will be unstable. The stability of haptic interactions can be defined in terms of energy dissipation and passivity theorem [13]. Since the passive systems cannot generate energy, this guarantees stable behavior of those systems. According to passivity theorem, a feedback connection of one passive system and one strictly passive

system is stable. It has many advantages for the analysis of coupled stability problems in haptic system that is coupled with human operator, haptic interface, and virtual environment [11]. We then use the following widely known definitions of passivity for a multi-port network.

Definition 1: (for continuous time system) The two-port network with initial energy storage *E(0)*, is passive, if and only if

$$\int_0^t \mathbf{f}(\tau)\cdot\mathbf{v}(\tau)d\tau + E(0) \geq 0, \quad \forall t \geq 0 \tag{13}$$

where $\mathbf{f}(\tau)$ and $\mathbf{v}(\tau)$ are continuous admissible forces and velocities, respectively.

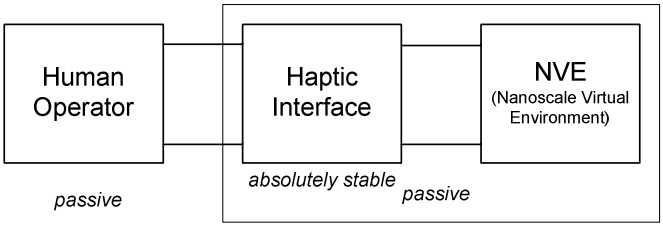

Fig. 8. Stable haptic simulation for tele-nanomanipulation

From Section II, it can be assumed that the human operator is passive. If the haptic interface and the NVE are also passive, then the total haptic simulation becomes stable as shown in Fig. 8. Therefore, the stability of the haptic simulation can be considered as the stability of one-port network.

Definition 2: (for sampled time system) The one-port network *N* with initial stored energy $E(0)$, is passive, if and only if [13]

$$E(k) = \sum_{\zeta=1}^{k} F(\zeta-1)\left[x(\zeta)-x(\zeta-1)\right] + E(0) \geq 0 \tag{14}$$

where $k = 1, 2, \ldots$, for sampled force $F(k)$ and position $x(k)$.

In this paper, the energy monitoring observer can be defined as,

$$\begin{aligned} E(k) = E(k-1) &+ f_c(k-1)\left[x_c(k)-x_c(k-1)\right] \\ &+ \gamma(k)\left[x_c(k)-x_c(k-1)\right] \end{aligned} \tag{15}$$

If the one-port system was not passive at step (*k*-1), the adaptive damper $\gamma(k)$ would be active for stability at step *k* as shown in Fig. 9. The $E(k-1) < 0$ means the system generates energy, and the amount of energy generated is $-E(k-1)$. Therefore, at step *k*, the active damper should be active for dissipating the generated energy $-E(k-1)$.

Assume that the initial energy $E(0) = 0$, and the one-port network system initially violates passivity condition at step (*k*-1). The $E(k-1)$ energy can be derived as

$$E(k-1) = \frac{\alpha_F}{\alpha_v}\sum_{\zeta=1}^{k-1} f_e(\zeta-1)\left[x_e'(\zeta)-x_e'(\zeta-1)\right] \tag{16}$$

where, $x_e'(k) = x_e(k) + x_{vc}(k)$.

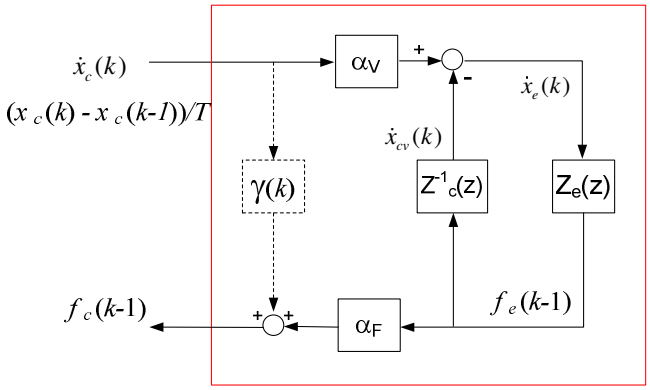

Fig. 9. One-port model with adaptive damper for sampled time passivity

Note that the ratio (α_F/α_v) in Eq. (16) is known as the *power scaling factor*. [18] Note also that the adaptive damper will be active for dissipating the generated energy whose amount is $-E(k-1)$ at step (*k*-1). To calculate the exact damper value at step *k*, we can derive the relationship between dissipated energy and the damper value as follows,

$$\gamma(k) = -\Delta E/\Delta x_c \tag{17}$$

where $\Delta x_c = x_c(k) - x_c(k-1)$ and $\Delta E = E(k-1)$.

D. Selection of Impedance Scaling Factor

We introduce the *characteristic length ratio* *k* and *k′* to represent the relationship between haptic, visual, and nano workspaces. For simplicity, we only consider the workspace as a cubic volume workspace. In addition, the distortions of workspace mapping are ignored. Note that the mapping between haptic device workspace and visual display workspace was considered as geometrical information mapping in Fig. 10. Note also that the concept of *characteristic length* is introduced for generalizing the specified trajectories of tasks. Moreover, the reachable and interested workspace for nanomanipulation with AFM could be considered as a cubic volume workspace in general.

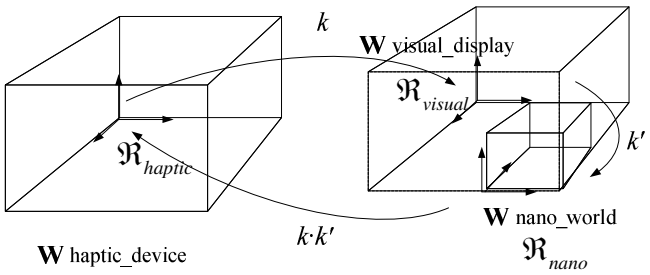

Fig. 10. The workspace mapping haptic device, visual display and nano world

The *characteristic length ratio* k can be expressed as

$$\frac{\mathbf{W}_{Haptic\_device}}{\mathbf{W}_{Visual\_display}} = \left(\frac{\ell_{Haptic\_device}}{\ell_{Visual\_display}} \right)^3 = k^3 \tag{18}$$

In a similar way, the *characteristic length ratio*, k', between visual display workspace and nano world workspace can be expressed as

$$k'^3 = \frac{\mathbf{W}_{Visual\_display}}{\mathbf{W}_{Nano\_world}} \tag{19}$$

If the visual display of the NVE is used to communicate with the operator magnifying the image of this real nano environment by certain factor $k \cdot k'$ that are shown in Fig. 10, then a good choice of the velocity scale factor is [18]

$$\alpha_v = \frac{1}{k \cdot k'} \tag{20}$$

Therefore, we can select the velocity (or position) scaling factor same as Eq. (20). Now, the selection of impedance scaling problem is thus reduced to finding the force scaling factor (α_F). From Eq. (11), to maximize *Z-width*, we should maximize the force scaling factor. However, Eq. (16) says that the generated energy magnifies with respect to the force scaling factor. This means that the selection of force scaling factor is a trade-off problem between impedance scaling and power scaling.

Goldfarb *et al.* [19] suggested the selection of a force scaling factor using dimensional analysis. For high surface adhesion, i.e. large AFM tip radius and high adhesion energy, $\alpha_F = 1/\alpha_v$ (Case I: dashed line in Fig. 11), and for small adhesion forces, $\alpha_F = 1/\alpha_v^2$ (Case II: bold line in Fig. 11) could give a better force feedback from his results. Fig. 11 represents that the *Z-width* is proportional to impedance scaling factor ($\alpha_v \alpha_F$). Note that depending on the task or the hardness of the sample, the force scaling factor should be chosen differently.

We derive the upper and lower bound of the force scaling factor based on Llewellyn's stability criteria [11]. Immittance matrix **P** of the two-port network system can be a hybrid matrix as in Eq. (7). Note that all gain (i.e. velocity scaling, virtual coupling) are fixed in this simulation. Immittance matrix **P** is *absolutely stable* if and only if

$$\begin{aligned} &\mathrm{Re}(p_{11}) \geq 0 \\ &2\,\mathrm{Re}(p_{11})\,\mathrm{Re}(p_{22}) \geq \left| p_{12} p_{21} \right| + \mathrm{Re}(p_{12} p_{21}) \end{aligned} \tag{21}$$

where

$$\mathbf{P} = \begin{bmatrix} Z_d(z) + \gamma \cdot ZOH(z) & \alpha_F \cdot ZOH(z) \\ -\alpha_v & \dfrac{1}{Z_c(z)} \end{bmatrix} = \begin{bmatrix} p_{11} & p_{12} \\ p_{21} & p_{22} \end{bmatrix}$$

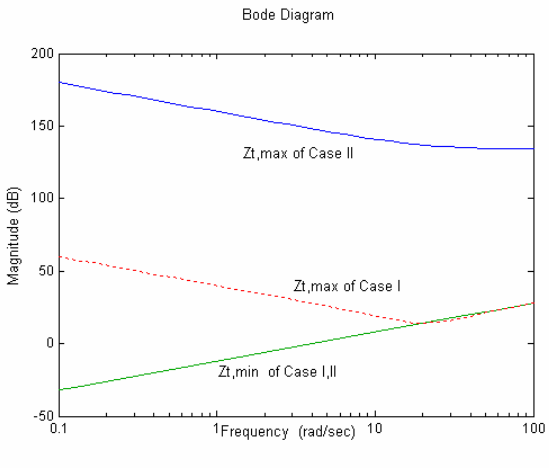

Fig. 11. *Z-width* with varying force scaling factor

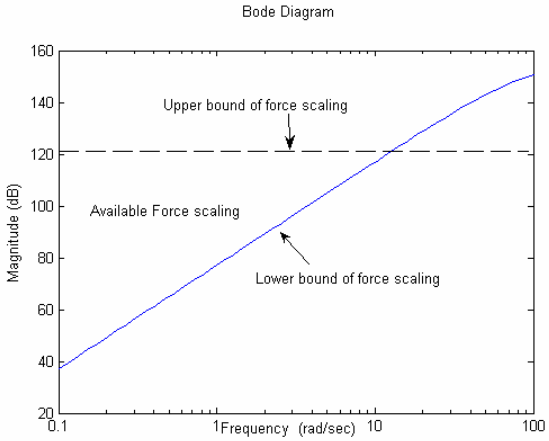

Fig. 12. Available region of force scaling factor based on absolute stability criteria and the physical limitation of the haptic device

Note that the physical limitation of the haptic device should be considered as following,

$$\alpha_F \leq \varepsilon \cdot \left| \hat{f}_a \right| / \left| \hat{f}_e \right| \tag{22}$$

where $\hat{f}_a$ and $\hat{f}_e$ are the maximum Cartesian forces of the haptic device and of the NVE, respectively, and ε $(0 < \varepsilon < 1)$ is the safety-factor of the haptic device. From Eq. (21) and (22), we find the available region of force scaling factor with guaranteed stability shown in Fig. 12.

IV. Experiments

As the first experiment, we tested the sampled time passivity controller for a stable haptic interface with the high stiffness contact sample such as silicon oxide in Table I. Fig. 13 represents the position and reflecting force of the haptic interface without a passivity controller. In comparison with Fig. 13, the passivity controller is active to stabilize the haptic interface shown in Fig. 14. The haptic interface could be stabilized in the NVE with the controller. Then, these control schemes can be used for tele-nanomanipulation with the haptic

device in the NVE.

Three types of tasks shown in Fig. 15 (a), (b) and (c) were performed with different samples (Table I). Task (a), shown in Fig. 15, requires positioning the AFM probe at a small distance (10~20nm) above the surface. Task (b) in Fig. 15 is positioning right on the surface and Task (c) is positioning below on the nano surface. Task (a) represents pushing carbon nanotubes or nanoparticles at a flat surface. This task requires holding the probe very close to but not touching the surface. Task (b) and (c) represent nanolithography and indenting shown in Fig. 16. This figure represents the nanoscale position and reflecting force when the specified nanoindentation tasks have been performed.

The sampled material properties of experiments are shown in Table I. One is the Young's modulus that represents the hardness of the material or the surface. Second is adhesion or surface energy of the surface; this factor determines how sticky the surface is. Finally, the Poisson's ratio is a ratio of the transverse strain to the normal strain of the material. Three different types of materials, from a hard surface (glass) to a soft surface (rubber), are used for our experiments. The results are presented in Fig. 17 and 18. In Fig. 18, the magnified figures show the interaction forces between the AFM tip and the sample at the transition between task (a) and task (b). Note that the interaction forces are very small to perceive. In the case of silicone rubber, its softness will give the operator less force feedback with same force scaling factor. The larger force scaling factor would be used for the soft rubber case within available force scaling region.

V. Conclusion

Task-based and stable tele-nanomanipulation in the NVE has been discussed in this paper. Nanoscale virtual coupling concept is introduced and the relationship between performance, stability, and scaling factors is explicitly derived. Based on Llewellyn's absolute stability criteria and the physical limitation of the haptic device, available force scaling region is presented. The sampled time domain passivity controller has been implemented for the stable haptic interface in the NVE. This controller has been used for three types of tasks with different samples with guaranteed stability. Experimental and simulation results show that the proposed stable haptic interface can be used for tele-nanomanipulation applications. During the experiments, non-contact force is so small compared to contact force that we cannot perceive the transition forces between non-contact and contact interacting in the NVE.

As future work, the developed stable haptic interface would be integrated with the AFM system as a slave manipulator for tele-nanomanipulation experiments. Experiments such as pushing a nano particle with precise positioning and nano assembly would be performed with stable haptic interaction. A new performance index would be developed for enhanced force reflecting perception of the non-contact forces during the specified task such as Fig. 15 (a). The sensitivity of non-contact forces with respect to distance from sample and the AFM tip may be used for the new performance index of the specific non-contact task.

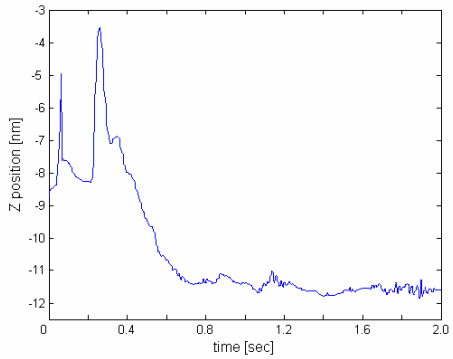

(a) z-position

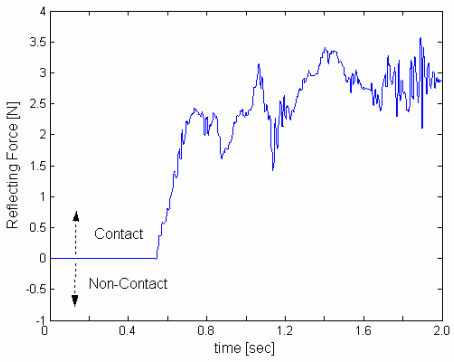

(b) Fz reflecting force

Fig. 13. Z-direction position and force without a time-domain passivity controller

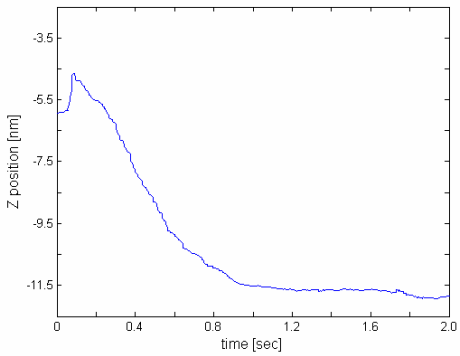

(a) z-position

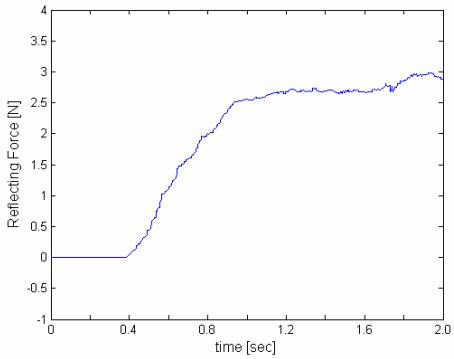

(b) Fz reflecting force

Fig. 14. Z-direction position and force with a time-domain passivity controller

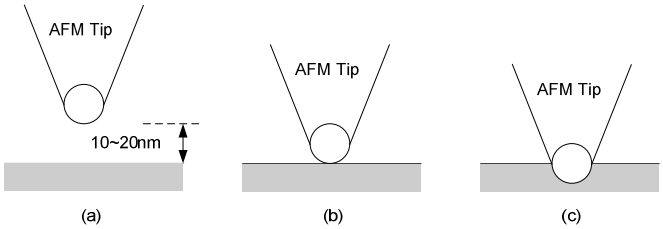

Fig. 15. Nanomanipulation tasks: (a) Small distance (10-20nm) above the nano sample surface, (b) Contact on the surface, and (c) Some distance below the surface (valid for only deformable surfaces)

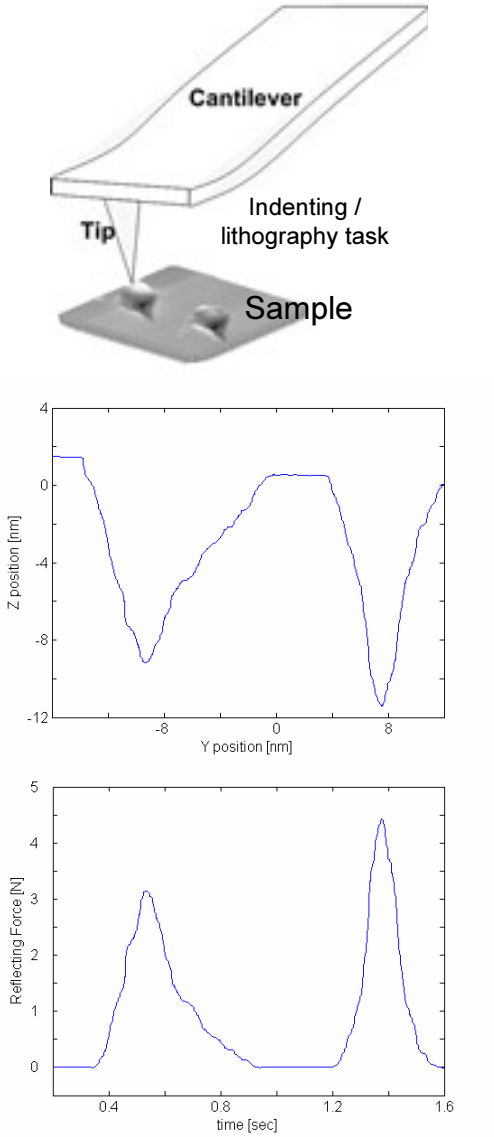

Fig. 16. Task (b) and (c) cases for nanoindentation in a NVE with the haptic interface

TABLE I
SAMPLED MATERIAL PROPERTIES [17]

Material	Young's Modulus (GPa)	Surface Energy (J/m^2)	Poisson's Ratio
Silicon Oxide	70	0.2	0.27
Polystyrene	2	0.066	0.4
Silicone Rubber (PDMS)	0.001	0.022	0.5

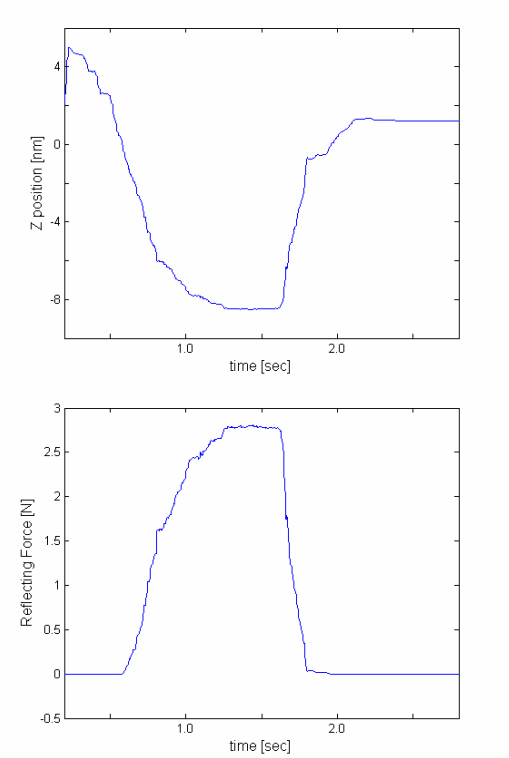

Fig. 17. Contact on a silicon oxide sample in a NVE with the haptic interface

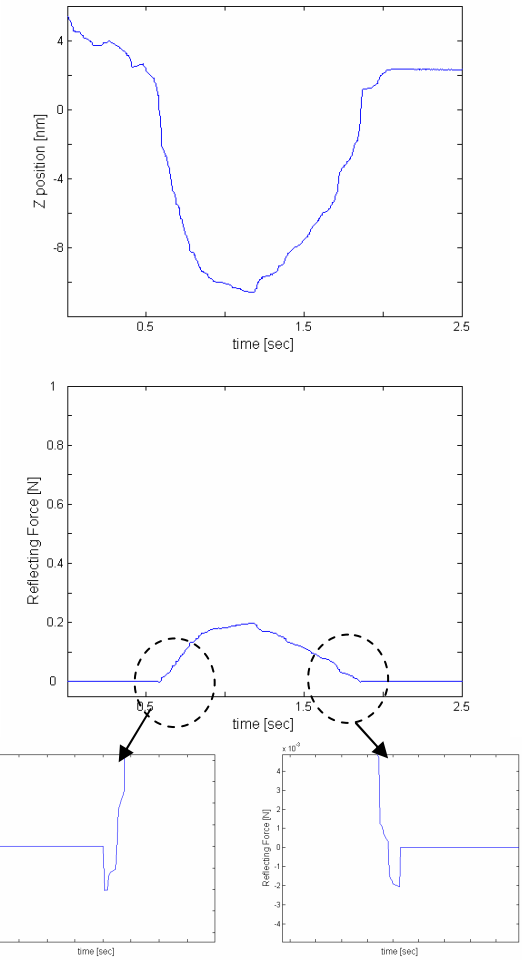

Fig. 18. Contact on a polystyrene sample in a NVE with the haptic interface

ACKNOWLEDGMENT

The authors would like to thank Wolfgang Vogl and Bernice Ma for developing the Virtual Reality user interface graphics and nanoforce simulator. This work was supported by the Postdoctoral Fellowship Program of the Korea Science and Engineering Foundation (KOSEF), and the NSF CAREER award program (NSF IIS-0448042).

REFERENCES

[1] M. Sitti and H. Hashimoto, "Teleoperated touch feedback from the surfaces at the nanoscale: modeling and experiments," *IEEE/ASME Trans. on Mechatronics*, vol. 8, no. 2, pp. 287-298, June 2003.

[2] R. L. Hollis, S. Salcudean, and D. W. Abraham, "Toward a tele-nanorobotic manipulation system with atomic scale force feedback and motion resolution," in *Proc. of the IEEE Int. Conf. Micro Electro Mechanical Systems*, pp. 115-119, 1990.

[3] M. Falvo *et al.*, "The nanoManipulator: A teleoperator for manipulating materials at the nanometer scale," in *Proc. of the Int. Symp. Science and Technology of Atomically Engineered Materials,* Richmond, VA, pp. 579-586, November 1995.

[4] M. Guthold *et al.*, "Controlled manipulation of molecular samples with the nanoManipulator," *IEEE/ASME Trans. on Mechatronics*, vol. 5, no. 2, pp. 189-198, June 2000.

[5] W. Vogl, M. Sitti, M. Ehrenstrasser, and M.F. Zäh, "Augmented Reality User Interface for Nanomanipulation using Atomic Force Microscopes," in *Proc. of the EuroHaptics 2004*, Technische Universitaet in Munich, Germany, June 2004.

[6] W. Vogl, *Telepresence at the Nano Scale: Augmented Reality Interface for Scanning Probe Microscopes*, Tech. Univ. of Munich, MSc Diploma Thesis, 2003.

[7] G. Li, N. Xi, M.Yu, and W.-K. Fung, "Development of augmented reality system for AFM-based nanomanipulation," *IEEE/ASME Trans. on Mechatronics*, vol. 9, no. 2, pp. 358-365, June 2004.

[8] A. S. Nain, D. H. Goldman, and M. Sitti, "Three-dimensional nanoscale manipulation and manufacturing using proximal probes: controlled pulling of polymer micro/nanofibers," in *Proc. of the IEEE Int. Conf. Robotics and Automation (ICRA 04)*, vol. 1, pp. 434-439, April 2004.

[9] G. Li, N. Xi, M.Yu, F. Salem, D. Wang, and J. Li, "Manipulation of Living Cells by Atomic Force Microscopy," in *Proc. of the IEEE/ASME Int. Conf. on Advanced Intelligent Mechatronics*, pp. 862-867, August 2003.

[10] J. E. Colgate and G. Schenkel, "Passivity of a class of sampled-data system: application to haptic interfaces," in *Proc. of the American Control Conf.*, pp. 3236-3240, Baltimore, 1994.

[11] R. J. Adams and B. Hannaford, "Stable haptic interaction with virtual environments," *IEEE Trans. on Robotics and Automation*, vol. 15, no. 3, pp. 465-474, June 1999.

[12] B. E. Miller, J. E. Colgate, and R. A. Freeman, "Guaranteed stability of haptic systems with nonlinear virtual environments," *IEEE Trans. on Robotics and Automation*, vol. 16, no. 6, pp. 712-719, December 2000.

[13] J.-H. Ryu, Y.-S. Kim, and B. Hannaford, "Sampled- and continuous – time passivity and stability of virtual environments," *IEEE Trans. on Robotics*, vol. 20, no. 4, pp. 772-776, August 2004.

[14] M.C. Cavusoglu, A. Sherman, and F. Tendick, "Design of bilateral teleoperation controllers for haptic exploration and telemanipulation of soft environments," *IEEE Trans. on Robotics and Automation*, vol. 18, no. 4, pp. 641 - 647, August 2002.

[15] J. E. Colgate and J. Brown, "Factors Affecting the Width of a Haptic Display," in *Proc. of the IEEE Int. Conf. Robotics and Automation (ICRA 94)*, IEEE CS Press, pp. 3205-3210, 1994.

[16] S. E. Salcudean *et al.*, "Bilateral matched impedance teleoperation with application to excavator control," *IEEE Control Systems Magazine*, vol. 19, no. 6, pp. 29-37, December 1999.

[17] G. Whitesides, E. Ostuni, S. Takayama, X. Jiang, and D. Ingber, "Soft Lithography in Biology and Biochemistry," *Annual Review of Biomedical Engineering*, vol. 3, pp.335-373, August 2001.

[18] J. E. Colgate, "Robust impedance shaping telemanipulation," *IEEE Trans. on Robotics and Automation*, vol. 9, no. 4, pp. 374-384, August 1993.

[19] M. Goldfarb, "Dimensional analysis and selective distortion in scaled bilateral telemanipulation," in *Proc. of the IEEE Int. Conf. Robotics and Automation (ICRA 98)*, Leuven, Belgium, pp.1609-1641, 1998.

[20] N. Hogan, "Controlling Impedance at the Man/Machine Interface," in *Proc. of the IEEE Int. Conf. Robotics and Automation*, vol. 3, Scottsdale, AZ, IEEE CS Press, pp. 1626-1631, 1989.